Analytic calculation of the radiance in an anisotropically scattering turbid medium close to a source

Rinzema, K.; Hoenders, B.J.; Ferwerda, H.A.; Bosch, J.J. ten

Published in:
Pure and Applied Optics

DOI:
10.1088/0963-9659/4/5/015

Pure Appl Opt. 4 (1995) 629–642. Printed in the UK

Analytic calculation of the radiance in an anisotropically scattering turbid medium close to a source

K Rinzema†§, B J Hoenders‡‖, H A Ferwerda‡¶ and J J Ten Bosch†

† Laboratory for Materia Technica, State University of Groningen, Bloemsingel 10, 9712 KZ Groningen, The Netherlands

‡ State University of Groningen, Department of Theoretical Physics, Nijenborgh 4, 9747 AG Groningen, The Netherlands

Received 5 December 1994, in final form 10 April 1995

Abstract. We present a method to calculate the radiance due to an isotropic point source in an infinite, homogeneous, anisotropically scattering medium. The method is an extension of a well known method for the case of isotropic scattering. Its basic mathematical ingredient is the Fourier transform. Its great advantage is that it also works very close to the source and not just far away from it, as is the case with most other methods. In principle, the method works for any phase function that can be expanded in a finite number of Legendre polynomials. Here, the simple example of linear anisotropic scattering is worked out numerically and the result is compared with Monte Carlo simulation. Good agreement is found between the two.

1. Introduction

Apart from the Monte Carlo method, nearly all theoretical methods used in tissue optics only work at a sufficiently large distance from the source and boundaries, diffusion theory being the most notable example [1–3]. The regime close to the source is, however, precisely the region where the radiance contains most information about the scattering characteristics of the medium. Moreover, it has been shown [4] that the diffuse reflection from a half-space illuminated by a pencil beam, originates predominantly from the region that is very close to the incoming beam. We try to study the spatial distribution of the radiance analytically because this gives a deeper insight than the Monte Carlo simulation, which is also often quite time consuming.

For the case of an isotropic point source in an unbounded, uniform, isotropically scattering medium a good approximation exists [5] which is good for small or large distances from the source and is fair throughout the whole medium. Unfortunately, it is not very useful for scattering in biological tissues which scatter highly anisotropically. In this paper we will extend the analysis to anisotropic scattering.

Although polarization of the light is an important feature if we are working in the non-diffusive area, it is seldom taken into account in biomedical applications and we do not consider it in this work either.

A similar remark can be made concerning coherence of the light, which has been discussed by MacKintosh and John [6]. These authors discuss both polarization and coherence effects.

§ E-mail address: K.RINZEMA@MED.RUG.NL
‖ E-mail address: HOENDERS@TH.RUG.NL
¶ E-mail address: FERWERDA@TH.RUG.NL

0963-9659/95/050629+14$19.50

2. Formulation of the problem

We consider an isotropic point source of unit strength in an unbounded, uniform anisotropically scattering medium.

When measuring lengths in units of the mean free path ($= (\mu_a + \mu_s)^{-1} = \rho\sigma_t$), in conventional notation) the equation of radiative transfer reads

$$\Omega \cdot \nabla L(r, \Omega) + L(r, \Omega) = a \int_{4\pi} L(r, \Omega') f(\Omega, \Omega')\, \mathrm{d}\Omega' + \delta(r) \tag{1}$$

where $L(r, \Omega)$ denotes the radiance, defined as the power which at position r is emitted through a unit area perpendicular to the direction denoted by the unit vector Ω. a is the albedo, defined as the ratio σ_s/σ_t of the scattering cross section σ_s and the total cross section σ_t. $f(\Omega, \Omega')$ is the phase function which gives the probability that a photon incident from the direction Ω is scattered into direction Ω'. Here we assume that the scatterer is not oriented; in that case the scattering function only depends on the angle between Ω and Ω'. $\delta(r)$ denotes the isotropic source of unit strength located at the origin of the coordinate system. The normalization of the phase function is taken to be

$$\int_{4\pi} f(\Omega, \Omega')\, \mathrm{d}\Omega' = 1\,. \tag{2}$$

The physics of the situation involves radial symmetry with respect to the origin. Therefore $L(r, \Omega)$ can only depend on the distance from the source, r, and the angle between the direction of r and Ω [7]:

$$L(r, \Omega) = L(r, \hat{r} \cdot \Omega) \tag{3}$$

where $r = |r|$ and $\hat{r}$ is the unit vector in the direction of r. This symmetry condition is fulfilled only because we consider unpolarized radiation.

We will show that the transport equation (1) can be solved by considering the Fourier transform $\mathcal{L}(k, \Omega)$ of $L(r, \Omega)$. To this end we multiply (1) by $\exp[-ik \cdot r]$ and integrate over r. Defining

$$\mathcal{L}(k, \Omega) = \int \mathrm{d}r\, L(r, \Omega) \exp[-ik \cdot r] \tag{4}$$

we find from (1)

$$(1 + ik \cdot \Omega)\mathcal{L}(k, \Omega) = a \int_{4\pi} \mathcal{L}(k, \Omega') f(\Omega, \Omega')\, \mathrm{d}\Omega'\,. \tag{5}$$

In the derivation we used the regularity of $L(r, \Omega)$ at infinity (see appendix A), but not the symmetry property (3). This symmetry property also leads to a corresponding symmetry for $\mathcal{L}(k, \Omega)$ (see equation (10)). This can be proved as follows: $L(r, \hat{r} \cdot \Omega)$ can be expanded in spherical harmonics:

$$L(r, \hat{r} \cdot \Omega) = \sum_{l=0}^{\infty} \sum_{m=-l}^{l} L_l(r) Y_{lm}(\Omega) Y_{lm}^*(\hat{r})\,. \tag{6}$$

The expansion of $\exp[-i\mathbf{k} \cdot r]$ in spherical harmonics reads

$$\exp[-i\mathbf{k} \cdot r] = \sum_{l=0}^{\infty} \sum_{m=-l}^{l} 4\pi (-\mathrm{i})^l j_l(kr) Y_{lm}^*(\hat{k}) Y_{lm}(\hat{r}) \tag{7}$$

where $\hat{k}$ is the unit vector in the direction of k. Substituting (6) and (7) into (4) and using the orthonormality property of $Y_{lm}(\hat{r})$ we find

$$\mathcal{L}(k, \Omega) = 4\pi \sum_{l=0}^{\infty} \sum_{m=-l}^{l} Y_{lm}^*(\hat{k}) Y_{lm}(\Omega) \mathcal{L}_l(k) \tag{8}$$

where

$$\mathcal{L}_l(k) = (-\mathrm{i})^l \int_0^{\infty} \mathrm{d}r\, r^2 j_l(kr) L_l(r)\,. \tag{9}$$

From equation (8) and the addition theorem for spherical harmonics we see that

$$\mathcal{L}(k, \Omega) = \mathcal{L}(k, \hat{k} \cdot \Omega) = \sum_{l=0}^{\infty} (2l+1) \mathcal{L}_l(k) P_l(\mu_\Omega) \tag{10}$$

where μ_Ω is the cosine of the angle between k and Ω. Thus, $\mathcal{L}(k, \Omega)$ only depends on $k = |k|$ and the angle between k and Ω.

We will now use (5) to derive an equation for $\mathcal{L}_l(k)$. To this end we need the expansion in spherical harmonics of $f(\Omega \cdot \Omega')$:

$$f(\Omega \cdot \Omega') = \sum_{l=0}^{N} \sum_{m=-l}^{l} f_l\, Y_{lm}(\Omega) Y_{lm}^*(\Omega') \tag{11}$$

where we assumed a *finite* summation over l. Substitution of (10) and (11) into (5) yields

$$\mathcal{L}(k, \mu_\Omega) = \frac{a}{2} \frac{1}{1 + \mathrm{i}k\mu_\Omega} \sum_{l=0}^{N} (2l+1) f_l \mathcal{L}_l(k) P_l(\mu_\Omega) + \frac{1}{2} \frac{1}{1 + \mathrm{i}k\mu_\Omega}\,. \tag{12}$$

Multiplying both sides of this equation by $P_l(\mu_\Omega)$ and integrating over μ_Ω leads to a set of linear equations for $\mathcal{L}_l(k)$:

$$\mathcal{L}_q(k) = \sum_{l=0}^{N} T_{ql}(k) \mathcal{L}_l(k) + S_q(k) \tag{13}$$

where we abbreviated

$$T_{ql}(k) = \tfrac{1}{2} a (2l+1) f_l \int_{-1}^{1} \mathrm{d}\mu_\Omega \frac{P_l(\mu_\Omega) P_q(\mu_\Omega)}{1 + \mathrm{i}k\mu_\Omega} \tag{14}$$

$$S_q(k) = \frac{1}{2} \int_{-1}^{1} \mathrm{d}\mu_\Omega \frac{P_q(\mu_\Omega)}{1 + \mathrm{i}k\mu_\Omega}\,. \tag{15}$$

The solution scheme is now as follows: equation (13) can be written as the matrix equation

$$\mathcal{L} = T\mathcal{L} + S \tag{16}$$

which can be solved by Cramer's rule:

$$\mathcal{L} = (I - T)^{-1} S \tag{17}$$

where I is the identity matrix. From $\mathcal{L}_l(k)$ we can deduce $L_l(r)$ by inverting (9), according to the Fourier–Bessel theory [8]:

$$L_l(r) = \frac{2\mathrm{i}^l}{\pi} \int_0^{\infty} \mathcal{L}_l(k) j_l(kr) k^2\, \mathrm{d}k\,. \tag{18}$$

When this program is completed we have from (6) the solution of our problem. In the following sections we will supply the details of the procedure.

3. Solution of the problem

The final step in the solution of the radiative transfer equation (1) is the determination of $L_l(r)$ using (18).

First we will show that the integration interval in (18) can be extended to $-\infty, +\infty$: from (9) we see that $\mathcal{L}_l(k)$ has odd (even) parity if l is odd (even), because of the same symmetry property of the spherical Bessel function $j_l(kr)$. Hence the integrand in (18) is even. Equation (18) can therefore be written as

$$L_l(r) = \frac{\mathrm{i}^l}{\pi} \int_{-\infty}^{+\infty} \mathcal{L}_l(k) j_l(kr) k^2 \, \mathrm{d}k \,. \tag{19}$$

We will calculate (19) by contour integration. To this end, it turns out to be convenient to consider the integral

$$\tilde{\Lambda}_l(r) = \frac{1}{\pi} \int_{-\infty}^{+\infty} \mathcal{L}_l(k) h_l^{(1)}(kr) k^2 \, \mathrm{d}k \tag{20}$$

where $h_l^{(1)}(kr)$ is the spherical Hankel function of the first kind: $h_l^{(1)}(kr) = j_l(kr) + \mathrm{i} y_l(kr)$. The integral in (19) is thus seen to be the real part of that in (20).

A useful representation of the function $h_l^{(1)}(z)$ is given by [9]

$$h_l^{(1)}(z) = \mathrm{i}^{-l-1} z^{-1} \exp(\mathrm{i}z) \sum_{k=0}^{l} \frac{(l+k)!}{k!(l-k)!} (-2\mathrm{i}z)^{-k} \,. \tag{21}$$

In appendix B it is shown that $\mathcal{L}_l(k)$ behaves asymptotically as $1/k$ for $k \to \pm\infty$. Because the functions $h_l^{(1)}(kr)$ behave asymptotically like $\mathrm{e}^{\mathrm{i}kr}/kr$, the integral in (21) appears to be divergent both at $k = \pm\infty$ and at $k = 0$. The divergence at $k = \pm\infty$ is already present in (19) and will turn out to give rise to a singularity at $r = 0$. At this stage we can still ignore this singularity for reasons that will become evident soon. The divergence at $k = 0$ has to be treated more carefully: the divergence is removed by subtracting the principal part of the Laurent expansion of $h_l^{(1)}(kr)$ at $k = 0$, $a_l(kr)$, from $h_l^{(1)}(kr)$. So instead of (20) we define $\Lambda(r)$ (without a tilde) as

$$\Lambda_l(r) = \frac{1}{\pi} \int_{-\infty}^{+\infty} \mathcal{L}_l(k) \{h_l^{(1)}(kr) - a_l(kr)\} \, \mathrm{d}k \,. \tag{22}$$

It should be noted that the subtraction of $a_l(kr)$ affects *neither* the real part of Λ_l, *nor* $L_l(r)$ because the principal part of $h_l^{(1)}(kr)$ is due to the (real-valued) spherical Neumann function $y_l(kr)$.

In appendix C we show that $\mathcal{L}_l(k)$ is a multi-valued function of k with branch points in $k = \pm\mathrm{i}$. The cut is chosen along the imaginary axis in the complex k-plane, extending from i to i∞ and from $-$i to $-$i∞ (figure 1).

We now calculate the integral in (22) by contour integration (figure 2). Let Γ be the contour in the complex k-plane consisting of the interval $[-R, +R]$ on the real axis ($R \to \infty$), four segments called γ_1 to γ_4, and two segments [i, i∞] on both sides of the cut, C_+ and C_-.

In appendix B it is shown that the contributions from the segments γ_2 and γ_3 tend to zero for $R \to \infty$ and also that the joint contribution due to the segments γ_1 and γ_4 oscillates about zero when $R \to \infty$, without actually becoming zero. We interpret this contribution as the mean value i.e. zero. This complication was to be expected because the integrals in (19) and (22) are 'mildly' divergent at $k = \pm\infty$. This divergence now manifests itself in the oscillatory contribution from γ_1 and γ_4.

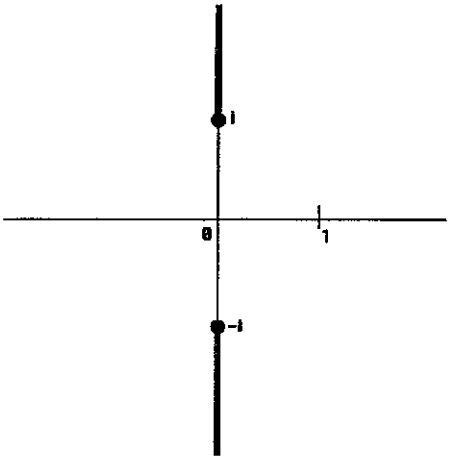

Figure 1. Cut in the complex k-plane, arising from the multi-valuedness of the functions $\mathcal{L}_l(k)$ (equations (22) and (C5)).

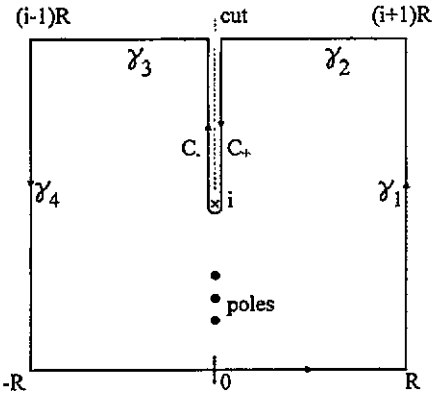

Figure 2. Integration contour Γ in the complex k-plane for the calculation of $L_l(r)$ (equation (23)).

From equation (17) it is to be expected that $\mathcal{L}_l(k)$ has poles inside Γ due to zeros of the determinant $|I - T|$. Let the residues in these poles be denoted by $\rho_1, \rho_2, \ldots, \rho_n$. Then

$$\oint_\Gamma \mathcal{L}_l(k)\{h_l^{(1)}(kr) - a_l(kr)\}k^2\,\mathrm{d}k = 2\pi\mathrm{i}\sum_{j=1}^{n}\rho_j\,. \tag{23}$$

The segments C_+ and C_- give the contributions from the cut. Denote $\mathcal{L}_l^+$ and $\mathcal{L}_l^-$ as the values of $\mathcal{L}_l(k)$ on the right and on the left of the cut, respectively. In this way we find, putting $k = \mathrm{i}s$,

$$\Lambda_l(r) = 2\mathrm{i}\sum_{j=1}^{n}\rho_j - \frac{1}{\pi}\int_1^\infty [\mathcal{L}_l^+(\mathrm{i}s) - \mathcal{L}_l^-(\mathrm{i}s)][h_l^{(1)}(\mathrm{i}sr) - a_l(\mathrm{i}sr)]s^2\,\mathrm{d}s\,. \tag{24}$$

The determination of the location and residues of the poles has to be done numerically. The integral in (24) can be expressed in terms of exponential integrals. Finally, the quantity of physical interest, $L_l(r)$ is obtained from the real part of (24).

The full procedure will be presented in a simple example to be discussed in the next section.

4. A simple example: linear anisotropic scattering

Linear anisotropic scattering refers to the phase function

$$f(\Omega \cdot \Omega') = \frac{1}{4\pi}(1 + 3g\cos\theta) \tag{25}$$

where g has to be less than $\frac{1}{3}$ in order to ensure the positive definiteness of f. The choice (25) corresponds to $f_0 = 1$ and $f_1 = g$.

The matrix elements T_{ql} are obtained from (14). The integrals in this equation are worked out in appendix C. Here the matrix elements are given in the form appropriate for use on both sides of the cut in the complex k-plane from i to i∞ (figure 2); '+' refers to the right-hand side of the cut, '−' refers to the left-hand side:

$$T_{00}^{\pm} = -\frac{1}{2}a\frac{\mathrm{i}}{k}\left\{\log\frac{1-\mathrm{i}/k}{1+\mathrm{i}/k} \bullet \pi\mathrm{i}\right\} \tag{26}$$

$$T_{01}^{\pm} = -\frac{3}{2}ag\left[2\frac{\mathrm{i}}{k} - \left(\frac{\mathrm{i}}{k}\right)^2\left\{\log\frac{1-\mathrm{i}/k}{1+\mathrm{i}/k} \pm \pi\mathrm{i}\right\}\right] \tag{27}$$

$$T_{10}^{\pm} = \frac{1}{3g}T_{01}^{\pm} \tag{28}$$

$$T_{11}^{\pm} = -\frac{3}{2}ag\frac{\mathrm{i}}{k}\left[2\frac{\mathrm{i}}{k} - \left(\frac{\mathrm{i}}{k}\right)^2\left\{\log\frac{1-\mathrm{i}/k}{1+\mathrm{i}/k} \pm \pi\mathrm{i}\right\}\right] \tag{29}$$

$$S_0^{\pm} = -\frac{1}{2}\left\{\log\frac{1-\mathrm{i}/k}{1+\mathrm{i}/k} \pm \pi\mathrm{i}\right\} \tag{30}$$

$$S_1^{\pm} = -\frac{\mathrm{i}}{k} - \frac{1}{2}\left(\frac{\mathrm{i}}{k}\right)^2\left\{\log\frac{1-\mathrm{i}/k}{1+\mathrm{i}/k} \pm \pi\mathrm{i}\right\}. \tag{31}$$

We now follow the procedure described in section 3 for this specific case. We start with $l = 0$. In that case (19) reads

$$L_0(r) = \frac{1}{\pi}\int_{-\infty}^{+\infty} \mathcal{L}_0(k)\, j_0(kr)k^2\,\mathrm{d}k\,. \tag{32}$$

This integral can be calculated by taking the real part of the following integral (note that $\mathcal{L}_0(k)$ is real according to (9)):

$$L_0^c(r) = \frac{1}{\pi}\int_{-\infty}^{+\infty} \mathcal{L}_0(k)(h_0^{(1)}(kr) - a_0(kr))\,k^2\,\mathrm{d}k \tag{33}$$

here $h_0^{(1)}(kr)$ is the spherical Hankel function of the first kind:

$$h_0^{(1)}(kr) = -\frac{\mathrm{i}}{kr}\mathrm{e}^{\mathrm{i}kr} \tag{34}$$

and $a_0(kr)$ is simply $-\mathrm{i}/(kr)$.

The integral in (33) can be calculated via the contour integral (see equation (23))

$$I_\Gamma = \frac{1}{\pi}\oint_\Gamma \mathcal{L}_0(k)h_0^{(1)}(kr)k^2\,\mathrm{d}k \tag{35}$$

$$= 2\mathrm{i}\sum_{j=1}^{n}\rho_j \tag{36}$$

Table 1. Zeros of the denominator $|I - T|$.

	g					
a	0.05	0.1	0.15	0.2	0.25	0.3
0.3	0.996	0.994	0.992	0.989	0.986	0.983
0.4	0.981	0.976	0.971	0.965	0.958	0.951
0.5	0.949	0.941	0.932	0.922	0.912	0.902
0.6	0.896	0.884	0.872	0.860	0.847	0.834
0.7	0.815	0.801	0.787	0.773	0.758	0.743
0.8	0.697	0.682	0.668	0.653	0.637	0.622
0.9	0.514	0.501	0.489	0.476	0.463	0.449

where Γ has been sketched in figure 2. The poles of the integrand are due to $\mathcal{L}_0(k)$, the residues of the integrand are denoted by ρ_j. $\mathcal{L}_0(k)$ is obtained from (17):

$$\mathcal{L}_0(k) = \frac{(1 - T_{11})S_0 + T_{01}S_1}{(1 - T_{11})(1 - T_{00}) - T_{01}T_{10}}. \tag{37}$$

The denominator of (37), $|I - T|$, may have zeros inside Γ which are poles of the integrand in (35). Numerically it turns out that for every combination of albedo a and anisotropy constant g there is one simple zero on the imaginary axis of the complex k-plane between 0 and $+\mathrm{i}$. This zero will be called ζ and has been tabulated in table 1.

The residue is found to be

$$\rho_0 = \frac{\mathrm{d}}{\mathrm{d}k}\mathcal{L}_0(k)\bigg|_{k=\zeta} h_0^{(1)}(\zeta r)\zeta^2 \tag{38}$$

which is purely imaginary when ζ is on the imaginary axis. For the evaluation of the contribution from the cut we expand $\mathcal{L}_0(k)$ in powers of i/k:

$$\mathcal{L}_0^{\pm}(k) = \sum_{n=1}^{\infty} \mathcal{L}_{0,n}^{\pm}\left(\frac{\mathrm{i}}{k}\right)^n \tag{39}$$

where the $\pm$ superscript refers to both sides of the cut. The analogue of (24) for this special case now reads

$$\begin{aligned} L_0^c(r) &= 2\mathrm{i}\rho_0 - \frac{\mathrm{i}}{\pi}\sum_{p=1}^{\infty}[\mathcal{L}_{0,p}^{+} - \mathcal{L}_{0,p}^{-}]\int_1^{\infty} s^{-p+1}\mathrm{e}^{-sr}\,\mathrm{d}s \\ &= 2\mathrm{i}\rho_0 - \frac{\mathrm{i}}{\pi r}\sum_{p=1}^{\infty}[\mathcal{L}_{0,p}^{+} - \mathcal{L}_{0,p}^{-}]E_{p-1}(r) \end{aligned} \tag{40}$$

where $E_n(r)$ is the exponential integral defined by

$$E_n(r) = \int_1^{\infty} \frac{\mathrm{e}^{-sr}}{s^n}\,\mathrm{d}s. \tag{41}$$

The leading term in (40) is given by $p = 1$. Upon calculation it appears that this is by far the most important term in (40). Thus, if we terminate the series in (40) at $p = 1$ we find after a straightforward but tedious calculation using $\mathcal{L}_{0,1}^{\pm} = \mp 1/2\pi\mathrm{i}$

$$L_0^c(r) = 2\mathrm{i}\rho_0 + \frac{1}{r^2}\mathrm{e}^{-r} \tag{42}$$

$$L_0(r) = \mathrm{Re}[2\mathrm{i}\rho_0] + \frac{\mathrm{e}^{-r}}{r^2} \tag{43}$$

or

$$L_0(r) = C\frac{e^{-\xi r}}{r} + \frac{e^{-r}}{r^2} \tag{44}$$

where C is a constant, to be determined from (38).

It is seen that the real-space radiance consists of two parts. In the literature [5] the first term in (44) is called the diffusive part and the second one the non-asymptotic part. Only for large distances from the source and for albedos close to unity we can neglect the non-asymptotic part.

The calculation of $L_1(r)$ proceeds entirely in the same way. Note that $\mathcal{L}_1(k)$ is purely imaginary because of (9). $L_1(r)$ is obtained by taking the real part of

$$L_1^c(r) = \frac{1}{\pi}\int_{-\infty}^{+\infty} i\mathcal{L}_1(k)(h_1^{(1)}(kr) - a_1(kr))\,k^2\,dk \tag{45}$$

where

$$h_1^{(1)}(kr) = -\frac{e^{ikr}}{kr}\left(1 + \frac{i}{kr}\right). \tag{46}$$

Proceeding in the same way as explained for $L_0(r)$ we find for the leading term using

$$\mathcal{L}_1 = \frac{T_{10}S_0 + (1 - T_{00})S_1}{(1 - T_{00})(1 - T_{11}) - T_{01}T_{10}} \tag{47}$$

$$\mathcal{L}_{1,1} = -1 \qquad \mathcal{L}_{1,2} = \mp\tfrac{1}{2}\pi i(1 - a) \tag{48}$$

$$L_1(r) = \mathrm{Re}[2i\rho_1] + \frac{1-a}{r}E_1(r) + \frac{1-a}{r^2}E_3(r) + \cdots \tag{49}$$

where ρ_1 is the residue of the integrand of (45) in the zero of the denominator of $\mathcal{L}_1(r)$ in (47). Again, as in the case of $L_0(r)$, the first term gives the diffusive part, and the other terms the non-asymptotic part.

The calculation of the angular moments $L_l(r)$ with $l > 1$, can be done in terms of the previously calculated quantities $\mathcal{L}_0$ and $\mathcal{L}_1$. This can be seen from (13) and (14) and from the fact that $f_l = 0$ for $l > 1$. Once the $\mathcal{L}_l(k)$ are known, the corresponding $L_l(r)$ can again be calculated by residue and branch-cut integration, analogous to the above.

As a check on our results we compared the calculated fluence rate to the outcome of a Monte Carlo simulation. The calculated fluence is simply $4\pi L_0(r)$, which can be seen by integrating (6) over all solid angles. The simulated fluence is the number of photons in a unit of volume, with no regard to their directions.

In the actual simulation we launched photons from the origin, in batches of 10 000. We let them propagate until a scattering event took place. Then we counted the total number of photons in each spherical shell of width $\Delta r = \frac{1}{20}$ (in units of scattering free path μ_s^{-1}). After that, a fraction $1 - a$ of the photons was 'killed' while the remainder survived and was propagated one more step, according to a linear anisotropic phase function. Meanwhile, a new batch of 10 000 was launched. The whole procedure was repeated until the total number of photons reached an equilibrium. When this was the case we compared the photon numbers to the result of (44) with an additional $p = 2$ term added (equation 40). It appeared that adding this term did not significantly alter the result, nor was this the case if any terms $p > 2$ were added.

The outcome is shown in figure 3. Here we used the values $a = 0.7$ and $g = 0.3$. The full circles are the numbers of photons obtained from the simulation. The full curve is the theoretical prediction of these numbers, up to second order in (i/k) (equation (40)). The

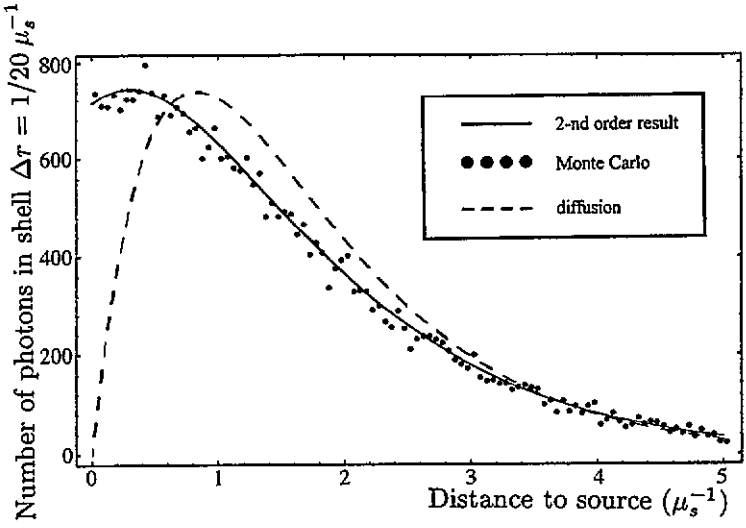

Figure 3. Comparison of second-order result in p (cf equation (40)) with Monte Carlo calculations.

agreement is quite satisfactory. Also shown (broken curve) is the result that would have been obtained from diffusion theory, namely [11], (equation (4))

$$L_0(r) = \frac{1}{Dr}\exp[-\mu_{eff}r]. \tag{50}$$

Here D and μ_{eff} involve the corrected transport cross section μ_{tr}, which is given by $\mu_{tr} = [\mu_a + \mu_s(1-g)]^{-1}$ [12] (equations (9)–(14)). In terms of the dimensionless quantities a and g they are given by

$$\mu_{eff} = [3(1-a)(1-ag)]^{1/2} \qquad \text{and} \qquad D = \frac{1-a}{\mu_{eff}^2}. \tag{51}$$

For small distances the approximation breaks down completely, as was to be expected. However, for large distances ($> 3\mu_s^{-1}$), equation (50) is seen to be a reasonable approximation for the real result. This implies that in this region the radiance has become diffuse, and therefore nearly isotropic.

Now, from the work of Dogariu and Asakura [13] it follows that the typical distance for the decay of polarization effects is about five transport mean free paths (μ_{tr}^{-1}), if the medium is not too densely packed. This suggests that polarization effects decay at least as slowly as anisotropy. Consequently, neglecting polarization is justifiable only as an intermediate step. Including it is certainly feasible, but not easy. Accordingly, neglecting it is common practice in most biomedical applications.

Acknowledgment

We are most indebted to J R Zijp for performing the Monte Carlo calculations.

Appendix A. Proof of a partial integration in section 1

In going from (1) to (5), we took some steps involving the operator ∇, which are not altogether straightforward. In fact we used

$$\int_V \mathrm{d}r\, \exp[-\mathrm{i}k\cdot r]\,(\Omega\cdot\nabla L(r,\Omega)) = -\int_V \mathrm{d}r\, L(r,\Omega)(\Omega\cdot\nabla)\exp[-\mathrm{i}k\cdot r] \tag{A1}$$

where V is the full three-dimensional space. This step can be justified as follows.

First from the product rule for differentiation we have for a general scalar field ϕ and vector field B:

$$\begin{aligned}\int_V \mathrm{d}r\,\phi(\nabla\cdot B) &= \int_V \mathrm{d}r\,\phi\,\partial_j B_j \\ &= \int_V \mathrm{d}r\,\partial_j(\phi B_j) - \int_V \mathrm{d}r\, B_j\partial_j\phi \\ &= \int_V \mathrm{d}r\,\nabla\cdot(\phi B) - \int_V \mathrm{d}r\,(B\cdot\nabla)\phi \end{aligned} \tag{A2}$$

in which we denoted the components of ∇ by ∂_j and adopted the summation convention. By Gauss' theorem, applied to the surface S of V, we can rewrite the first term on the right hand side of (A2) as $\int_V \mathrm{d}r\,\nabla\cdot(\phi B) = \int_S \phi(B\cdot\mathrm{d}\vec{\sigma})$, where $\vec{\sigma}$ is directed along the outward normal on the surface element $\mathrm{d}\sigma$. As Ω is a constant vector, $L\cdot\nabla\Omega = 0$ and hence

$$\Omega\cdot\nabla L = \nabla\cdot(\Omega L)\,. \tag{A3}$$

If we regard $\Omega L(r,\Omega)$ as one vector field and use equations (A1) and (A2), we find that

$$\begin{aligned}&\int_V \mathrm{d}r\,\exp[-\mathrm{i}k\cdot r]\,\Omega\cdot\nabla L(r,\Omega) \\ &\quad= \int_V \mathrm{d}r\,\exp[-\mathrm{i}k\cdot r]\,\nabla\cdot(\Omega L(r,\Omega)) \\ &\quad= \int_S \exp[-\mathrm{i}k\cdot r]\,((\Omega L(r,\Omega)\cdot\mathrm{d}\vec{\sigma}) - \int_V \mathrm{d}r\, L(r,\Omega)(\Omega\cdot\nabla)\exp[-\mathrm{i}k\cdot r]\,.\end{aligned} \tag{A4}$$

Assuming that $L(r,\Omega)$ decreases sufficiently fast for large distances, we see that the surface integral vanishes, which proves (A1).

Appendix B. Interpretation of the divergent integral in (19)

In this section we will investigate the large-k behaviour of $\mathcal{L}_l(k)$ and the way it affects the inverse Fourier–Bessel transform. For $\mathcal{L}_l(k)$ we had (17)

$$\mathcal{L} = (I-T)^{-1}S\,. \tag{B1}$$

From equation (14) it is easy to see that for large $|k|$ the matrix elements of T tend to zero. Hence, from equation (B1), we see that to order $1/k$, $\mathcal{L}_l(k)$ behaves like $S_l(k)$, i.e.

$$\mathcal{L}_l(k) = S_l(k) + \mathrm{O}(k^{-2}) \qquad \text{for} \quad |k|\to\infty\,. \tag{B2}$$

The asymptotic behaviour of $S_l(k)$ can be obtained from its integral representation (15). Thus, (see figure 4)

$$S_l(k) = \frac{1}{2}\int_{-1}^{1}\frac{P_l(\mu)}{1+\mathrm{i}k\mu}\mathrm{d}\mu$$

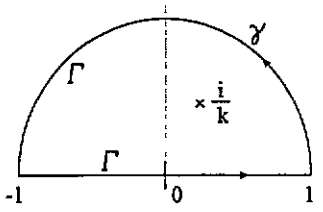

Figure A1. Integration contour in the complex μ-plane for the derivation of the asymptotic behaviour of $S_l(k)$ and $\mathcal{L}_l(k)$ (equation (B3))

$$= \frac{1}{2}\oint_{\Gamma} \frac{P_l(\mu)}{1+\mathrm{i}k\mu}\mathrm{d}\mu - \frac{1}{2}\int_{\gamma} \frac{P_l(\mu)}{1+\mathrm{i}k\mu}\mathrm{d}\mu \tag{B3}$$

where Γ is the entire closed contour in figure 4 and γ is only the semicircle. The first integral yields, by the theorem of residues

$$-\frac{1}{2}\frac{\mathrm{i}}{k}\oint_{\Gamma} \frac{P_l(\mu)}{\mu-\mathrm{i}/k}\mathrm{d}\mu = \frac{\pi}{k}P_l\left(\frac{\mathrm{i}}{k}\right) \qquad \mathrm{Re}\,k > 0 \tag{B4}$$

$$= 0 \qquad \mathrm{Re}\,k < 0\,. \tag{B5}$$

In the second term of equation (B3), we put $\mu = \mathrm{e}^{\mathrm{i}\phi}$ and expand the fraction to get

$$\begin{aligned} -\frac{1}{2}\int_{\gamma} \frac{P_l(\mu)}{1+\mathrm{i}k\mu}\mathrm{d}\mu &= \frac{\mathrm{i}}{2}\int_0^{\pi}\left(\frac{\mathrm{i}}{k}\right)\frac{P_l(\mathrm{e}^{\mathrm{i}\phi})}{1-(\mathrm{i}/k)\mathrm{e}^{-\mathrm{i}\phi}}\mathrm{d}\phi \\ &= -\frac{1}{2k}\int_0^{\pi} P_l(\mathrm{e}^{\mathrm{i}\phi})\sum_{n=0}^{\infty}\left(\frac{\mathrm{i}}{k}\right)^n \mathrm{e}^{-\mathrm{i}n\phi}\,\mathrm{d}\phi \\ &= -\frac{1}{2k}\int_0^{\pi} P_l(\mathrm{e}^{\mathrm{i}\phi})\,\mathrm{d}\phi + \mathrm{O}(k^{-2}) \qquad |k| \to \infty\,. \end{aligned} \tag{B6}$$

The results are different according as l is even or odd.

For odd l, the first term in (B3) is only of order k^{-2}, or zero. The second term follows from equation (B6). Thus

$$\lim_{|k|\to\infty}\frac{1}{2}\int_{-1}^{1}\frac{P_l(\mu)}{1+\mathrm{i}k\mu}\mathrm{d}\mu = \frac{\pi}{2k}\int_0^{\pi} P_l(\mathrm{e}^{\mathrm{i}\phi})\,\mathrm{d}\phi + \mathrm{O}(k^{-2})\,. \tag{B7}$$

For even l, the procedure is analogous, but now the first term in equation (B3) also contributes. From equations (B4) and (B5) we see that this contribution is either $(\pi/k)P_l(0)$ or 0. For the second term we find from (B6)

$$\begin{aligned} \lim_{|k|\to\infty}\frac{1}{2}\int_{\gamma}\frac{P_l(\mu)}{1+\mathrm{i}k\mu}\mathrm{d}\mu + \mathrm{O}(k^{-2}) &= \frac{\pi}{2k}\int_0^{\pi} P_l(\mathrm{e}^{\mathrm{i}\phi})\,\mathrm{d}\phi \\ &= \frac{\pi}{2k}P_l(0) + \mathrm{O}(k^{-2}) \end{aligned} \tag{B8}$$

where the last line follows, because for even l all terms in $P_l(\mathrm{e}^{\mathrm{i}\phi})$ are an even power of $\mathrm{e}^{\mathrm{i}\phi}$. Hence, in the integral only the zero-degree term survives and gives $2\pi\,P_l(0)$. Hence, from (B3)–(B6) and (B8) we have

$$\lim_{|k|\to\infty}\frac{1}{2}\int_{-1}^{1}\frac{P_l(\mu)}{1+\mathrm{i}k\mu}\mathrm{d}\mu = +\frac{\pi}{2k}P_l(0) + \mathrm{O}(k^{-2}) \qquad \mathrm{Re}\,k > 0 \tag{B9}$$

$$= -\frac{\pi}{2k}P_l(0) + \mathrm{O}(k^{-2}) \qquad \mathrm{Re}\,k < 0\,. \tag{B10}$$

We see that both for l even and for l odd, $S_l(\frac{1}{k})$ and therefore also $\mathcal{L}_l(k)$ behave asymptotically like $1/k$. However, for even l there is a change in sign, according as $\mathrm{Re}\,k$ is either > 0 or < 0

The real-space radiance was given by (19) and (20)

$$L_l(r) = \mathrm{Re}\,\frac{\mathrm{i}^l}{\pi}\int_{-\infty}^{+\infty}\mathcal{L}_l(k)(h_l^{(1)}(kr) - a_l(kr))\,k^2\,\mathrm{d}k\,. \tag{B11}$$

If we use that $h_l^{(1)}(kr)$ behaves asymptotically like $\frac{\mathrm{i}}{kr}\mathrm{e}^{\mathrm{i}kr}(-\mathrm{i})^l$ and the asymptotic behaviour of $\mathcal{L}_l(k)$, deduced above, we see that the integral in (B11) is divergent for $k \to \pm\infty$. To get around this, we consider the principal value of the integral and assign to $L_l(r)$ the value around which this oscillates as the limits in the integral tend to infinity, i.e.

$$L_l(r) = \mathrm{Re}\,\frac{\mathrm{i}^l}{\pi}\lim_{R\to\infty}\int_{-R}^{+R}\mathcal{L}_l(k)(h_l^{(1)}(kr) - a_l(kr))\,k^2\,\mathrm{d}k\,. \tag{B12}$$

To justify the use of the contour in section 4, we now calculate the contributions due to γ_1-γ_4. Because for s large and positive, $h_l^{(1)}(\mathrm{i}sr)$ behaves like e^{-sr}/sr, the contributions due to γ_2 and γ_3 vanish. For that due to γ_1 we have for even l (from equations (B9) and (B10))

$$\lim_{R\to\infty}\frac{\mathrm{i}^l}{\pi}\int_{\gamma_1}\mathcal{L}_l(k)\,(h_l^{(1)}(kr) - a_l(kr))k^2\,\mathrm{d}k = \lim_{R\to\infty}\int_R^{(1+\mathrm{i})R}\frac{P_l(0)}{r}\mathrm{e}^{\mathrm{i}kr}\,\mathrm{d}k$$

$$= \frac{P_l(0)}{\mathrm{i}r^2}\,(\mathrm{e}^{(\mathrm{i}-1)rR} - \mathrm{e}^{\mathrm{i}rR})\,. \tag{B13}$$

Similarly, the contribution of γ_4 is for even l

$$\lim_{R\to\infty}\int_{-R}^{(\mathrm{i}-1)R}\frac{P_l(0)}{r}\mathrm{e}^{\mathrm{i}kr}\,\mathrm{d}k = -\frac{P_l(0)}{\mathrm{i}r^2}\,(\mathrm{e}^{-\mathrm{i}rR} - \mathrm{e}^{-(\mathrm{i}+1)rR})\,. \tag{B14}$$

Adding these results together, for the joint contribution we find

$$\lim_{R\to\infty}\frac{\mathrm{i}^l}{\pi}\int_{\gamma_1\cup\gamma_4}\mathcal{L}_l(k)\,(h_l^{(1)}(kr) - a_l(kr))k^2\,\mathrm{d}k = \frac{2\mathrm{i}}{r^2}P_l(0)\,(-1+\mathrm{e}^{-Rr})\cos rR\,. \tag{B15}$$

We interpret this result as the mean value around which it keeps oscillating as $R \to \infty$, and for $r \neq 0$ this is seen to be zero. This is called interpretation in the Cesàro sense. Thus interpreted, the contribution of γ_1-γ_4 is therefore zero, as was assumed in the main text.

A completely similar argument holds if l is odd.

Appendix C. Analytic properties of the integrals in (14) and (15)

We will study the integrals

$$\int_{-1}^{1}\frac{P_n(u)}{1+\mathrm{i}ku}\mathrm{d}u \tag{C1}$$

and

$$\int_{-1}^{1}\frac{P_n(u)P_m(u)}{1+\mathrm{i}ku}\mathrm{d}u\,. \tag{C2}$$

Both integrals represent functions in the complex k-domain with branch points in $k = \pm i$. This can be shown simply and explicitly by considering the integral

$$I_n = \int_{-1}^{1} \frac{u^n}{1 + iku} du . \tag{C3}$$

Without actually calculating this integral we see that I_n is positive if k lies on the imaginary axis between $-i$ and $+i$. So there the argument of I_n can be chosen to be zero. The integral can also be calculated explicitly:

$$I_n = \sum_{j=0}^{n-1} C_j^n \frac{(-1)^j}{(n-j)(ik)^{n-j}} \{(1+ik)^{n-j} - (1-ik)^{n-j}\} + \frac{(-1)^n}{(ik)^{n+1}} \{\log(1+ik) - \log(1-ik)\} \tag{C4}$$

where C_j^n is the combinatorial factor $n!/(n-j)!j!$ Now we have to choose the appropriate branch for the logarithm: as I_n is positive for imaginary values of k between $-i$ and $+i$, we write

$$\frac{(-1)^n}{(ik)^{n+1}} \{\log(1+ik) - \log(1-ik)\} = \frac{(-1)^n}{(ik)^{n+1}} \log \frac{1+ik}{1-ik} \tag{C5}$$

where the principal branch of the logarithm has been chosen for k between $-i$ and $+i$. So the cuts in the complex plane have to be chosen as sketched in figure 1. The argument of the multi-valued function contained in I_n is therefore $+\pi$ on the right-hand side of the cut starting at $+i$ and $-\pi$ on its left-hand side.

The integrals to be studied in this appendix are known and involve the function $Q_n(z)$ [14], which for $-1 < z < 1$ is given by

$$Q_n(z) = \frac{1}{2} P_n(z) \log \frac{1-z}{1+z} + W_{n-1}(z) . \tag{C6}$$

This is actually the arithmetic mean of the values immediately above and below the cut which, in the complex z-plane, runs from -1 to 1. In accordance with the above, we have for k immediately to the right of the cut in the k-plane

$$Q_n\left(\frac{i}{k}\right) = \frac{1}{2} P_n\left(\frac{i}{k}\right) \left[\log \frac{1 - i/k}{1 + i/k} + \pi i\right] + W_{n-1}\left(\frac{i}{k}\right) . \tag{C7}$$

Here, $W_{n-1}(z)$ is a polynomial in z of degree $n-1$ with real coefficients, which will not be specified any further.

References

[1] Groenhuis R A J, Ferwerda H A and Ten Bosch J J 1983 Scattering and absorption of turbid materials determined from reflection measurements 1. *Appl. Opt.* **22** 2456–60

[2] Patterson M S, Wilson B C and Wyman D R 1991 The propagation of optical radiation in tissue I. *Lasers Med. Sci.* **6** 155–68

[3] Farrell T J, Patterson M S and Wilson B C 1992 A diffusion theory model of spatially resolved, steady state diffuse reflectance for the noninvasive determination of tissue optical properties *in vivo Med. Phys.* **19** 879–88

[4] Bolt R A and Ten Bosch J J 1994 On the determination of optical parameters for turbid materials *Waves Random Media* **4** 233–42

[5] Case K M, de Hoffman F and Placzek G 1953 *Introduction to the Theory of Neutron Diffusion* vol I (Washington DC: US Government Printing Office)

[6] MacKintosh F C and John S 1989 Diffusing-wave spectroscopy and multiple scattering of light in correlated random media *Phys. Rev.* B 40 2383–406

[7] Davison B and Sykes J B 1957 *Neutron Transport Theory* (Oxford: Clarendon) section 11.1

[8] Korn G and Korn T 1968 *Mathematical Handbook for Scientists and Engineers* (New York: McGraw-Hill) formulae 8.6–13 and 21.8–39

[9] Abramowitz M and Stegun I A 1972 *Handbook of Mathematical Functions* (New York: Dover) formula 10.1.16

[10] Courant R and Hilbert D 1953 *Methods of Mathematical Physics* vol 1 (New York: Interscience) p 534

[11] Patterson M S, Schwartz E and Wilson B C 1989 Quantitative reflectance spectroscopy for the noninvasive measurement of photosensitizer concentration in tissue during photodynamic therapy *SPIE* vol 1065 *Photodynamic Therapy: Mechanisms* pp 115–22

[12] Ishimaru A 1978 *Wave Propagation and Scattering in Random Media* vol 1 (New York: Academic)

[13] Dogariu M and Asakura T 1993 Polarization dependent backscattering patterns from weakly scattering media *J. Opt.* 24 271–8

[14] Gradshteyn I S and Ryzhik I M 1981 *Table of Integrals, Series and Products* (corrected and enlarged edition) (New York: Academic) formula 8.831.2